Available online at www.sciencedirect.com

SCIENCE DIRECT®

Catalysis Today 106 (2005) 41–46

CATALYSIS TODAY

www.elsevier.com/locate/cattod

Sorption enhanced hydrogen production by steam methane reforming using Li_2ZrO_3 as sorbent: Sorption kinetics and reactor simulation

Esther Ochoa-Fernández, Hans Kristian Rusten, Hugo Atle Jakobsen, Magnus Rønning, Anders Holmen, De Chen *

Department of Chemical Engineering, Norwegian University of Science and Technology (NTNU), N-7491 Trondheim, Norway

Abstract

The kinetics of CO_2 sorption on a solid adsorbent, namely lithium zirconate, have been studied in an oscillating microbalance. The solid sorbent has been prepared by a novel route resulting in a high capacity, good stability and much improved sorption rates, making it suitable for its application in sorption enhanced hydrogen production by steam methane reforming. A kinetic equation for the sorption kinetics as a function of CO_2 partial pressure and temperature has been developed. The hydrogen production by sorption enhanced reaction process has been simulated by a dynamic one-dimensional pseudo-homogenous model of a fixed-bed reactor, where a hydrotalcite-derived Ni catalyst has been used as steam reforming catalysts. Simulation results show that hydrogen purer than 95% with a concentration of carbon monoxide lower than 0.2 mol% can be produced in a single step.

Keywords: CO_2 sorption; H_2 production; Lithium zirconate; Enhanced steam reforming; Ni

1. Introduction

The issue of global warming is becoming a major element in the world energy policy. Presently, about 29 billion tonnes of CO_2 are released into the air annually by human activities, including 23 billion from fossil fuels burning and industry. According to the Kyoto protocol, this emission has to be dramatically reduced and it is then imperative to give high priority to the sequestration of CO_2 and efficient power generation [1].

Many studies have recently been carried out related to the CO_2 removal from flue gases. Currently available technologies for CO_2 separation include: physical and chemical absorption [2], physical and chemical adsorption [3], cryogenic processes and gas separation membranes [4]. Recently, special attention has been given to the use of lithium zirconate as CO_2 adsorbent at high temperatures [5–10]. Nakagawa and Ohashi [5,6] have reported that lithium zirconate can theoretically adsorb CO_2 in amounts up to 28% adsorbent weight at high temperatures according to the following reaction:

$$Li_2ZrO_3 + CO_2 \leftrightarrow Li_2CO_3 + ZrO_2;\quad \Delta H\,(298\,\mathrm{K}) = -160\,\mathrm{kJ/mol} \qquad (1)$$

The high adsorption capacity and stability of this material make it increasingly promising for this purpose. However, kinetic limitations are still the main drawback.

The removal of CO_2 from hot gas streams is becoming very significant in the field of energy production. For example, the novel sorption enhanced reaction process (SERP) has the potential to decrease the cost of hydrogen production by steam methane reforming [11]. In this process, a CO_2 acceptor is installed together with the catalyst for removal of CO_2 from the gas phase and hence pushing the equilibrium limits for the reforming and water–gas shift reactions. It is possible to obtain a product containing as much as 97% H_2 (dry basis) [11]. The steam reforming can be run at much lower temperatures

---

* Corresponding author. Tel.: +47 43 73593149; fax: +47 43 73595047.
E-mail address: chen@chemeng.ntnu.no (D. Chen).

0920-5861/$ – see front matter © 2005 Elsevier B.V. All rights reserved.
doi:10.1016/j.cattod.2005.07.146

Nomenclature

C	concentration (mol/m^3)
Cp_g	heat capacity of gas (J/mol K)
Cp_s	heat capacity of solid (J/mol K)
d_p	particle diameter (m)
d_t	internal reactor diameter
D_L	effective axial dispersion coefficient (m^2/s)
D_m	molecular diffusivity (m^2/s)
E_{ad}	energy of adsorption (J/mol)
ΔH_j	enthalpy of the reaction j (kJ/mol)
k_{ad}	rate constant for the adsorption
K_D	Ergun equation coefficient (N s/m^4)
K_V	Ergun equation coefficient (N s^2/m^5)
L	length of reactor (m)
M_i	molecular weight of i (g/mol)
n	exponent in the sorption kinetics equation
N_f	total reactor feed (mol/s)
P	total pressure in reactor (Pa)
P_{CO_2}	partial pressure of CO_2 (atm)
P_f	total pressure in reactor feed (Pa)
Pr	Prandtl's number
r_{ad}	sorption rate (mol/kg s)
R	gas constant (J/mol K)
R_i	catalytic reaction rate reaction i (mol/kg s)
Re_p	Reynolds number, based on particle
t	time (s)
T	temperature (K)
T_f	feed temperature (K)
T_w	wall temperature (K)
u	superficial gas velocity (m/s)
U	overall bed-wall heat transfer coefficient (J/m^{2}K)
Δw	uptake of CO_2 (g CO_2/g absorbent)
x	extent of reaction
y_i	mole fractions of component i
y_{fi}	mole fractions of component i in feed
z	axial position (m)

Greek symbols

ε	void fraction in reactor
η_j	effectiveness factor of reaction j
λ_g	gas conductivity (W/mK)
λ_p	solid conductivity (W/mK)
λ_z	effective axial conductivity (W/mK)
μ	gas viscosity (Pa s)
ν_{ij}	stochiometric factor of component i in reaction j
ρ_b	density of the bed (adsorbent + catalyst) (kg/m^3)
$\rho_{b,ad}$	bed density of adsorbent (kg/m^3)
$\rho_{b,cat}$	bed density of catalyst (kg/m^3)
ρ_g	density of gas (kg/m^3)

(723–903 K) than conventional steam reforming. As a result, investment and operation costs are significantly reduced. The key reactions of the process are the steam methane reforming (SMR) and the water–gas shift reaction:

$$CH_4 + H_2O \leftrightarrow CO + 3H_2;\quad \Delta H\,(298\,\mathrm{K}) = 206\,\mathrm{kJ/mol} \tag{2}$$

$$CO + H_2O \leftrightarrow CO_2 + H_2;\quad \Delta H\,(298\,\mathrm{K}) = -41\,\mathrm{kJ/mol} \tag{3}$$

$$CH_4 + 2H_2O \leftrightarrow CO_2 + 4H_2;\quad \Delta H\,(298\,\mathrm{K}) = 165\,\mathrm{kJ/mol} \tag{4}$$

In this work, we have used Li_2ZrO_3 to adsorb CO_2 during the reaction aiming to produce hydrogen with purity higher than 95%. The reported sorption rates of CO_2 on Li_2ZrO_3 are too low for enhanced steam reforming. However, a novel soft chemical method has recently been developed in our laboratory, which can significantly improve the CO_2 sorption kinetics of lithium zirconate. The present work deals with a kinetic study of CO_2 sorption using a tapered element oscillating microbalance (TEOM) [15]. The purpose has been to determine a kinetic equation for sorption of CO_2 and to use this kinetic equation in a fixed-bed reactor model in order to simulate the hydrogen production according to the SERP concept. A hydrotalcite derived Ni catalyst has been used as steam reforming catalyst [12].

2. Experimental

The solid sorbent, namely lithium zirconate, has been prepared by means of a novel soft chemical method in our laboratory [13]. The crystalline structure of the prepared sample was characterised by X-ray diffraction (XRD) analysis using Cu Kα radiation. The crystallite size was calculated using the Scherrer equation [14].

CO_2 sorption properties were evaluated using a tapered element oscillating microbalance [15]. The tapered element was loaded with 20 mg of Li_2ZrO_3 together with quartz particles. The samples were heated to 823–873 K with a heating rate of 10 K/min in pure Ar and kept for 60 min at atmospheric pressure. The CO_2 sorption was started by switching from Ar to a mixture of CO_2 and Ar while maintaining the temperature. The flow rates of Ar and the mixture were kept constant at 100 ml/min. After saturation of the adsorbent, the temperature was increased to 953 K and the flow gas was changed from CO_2/Ar mixture to Ar to proceed with the desorption reaction. The experiments were carried out at different CO_2 partial pressures and sorption temperatures. The different partial pressures of CO_2 were obtained by adjusting flow rates of CO_2 and Ar at a constant total flow rate of 100 ml/min.

3. Kinetic modelling and reactor simulation

In order to use the experimental results from the TEOM measurements in a mathematical reactor model for the SERP, a mathematical model for the adsorption had to be developed. Since the experimental conditions have been selected as differential conditions, the TEOM reactor can be simply simulated as a differential reactor. The model chosen is of the form:

$$\frac{\mathrm{d}x}{\mathrm{d}t} = k_{\mathrm{ad}} C^{n}_{\mathrm{CO_2}}(1-x) \tag{5}$$

x is the extent of reaction, defined as $x = \Delta w/\Delta w_{\max}$, where the maximum experimental uptake of CO_2, $\Delta w_{\max}$, is set to 0.22 g CO_2/g adsorbent.

The sorption reaction rate can then be expressed as:

$$r_{\mathrm{ad}} = \frac{\Delta w_{\max}}{M_{\mathrm{CO_2}}}\frac{\mathrm{d}x}{\mathrm{d}t} \tag{6}$$

The temperature dependence of k_{ad} is given by:

$$k_{\mathrm{ad}} = k^{0}_{\mathrm{ad}} \mathrm{e}^{-E_{\mathrm{ad}}/R(1/T-1/T_0)}; \quad \text{where } T_0 \text{ is } 848\,\mathrm{K}. \tag{7}$$

A dynamic one-dimensional pseudo-homogenous model has been formulated for simulation of the reactor for SERP. The following assumptions are made: axially dispersed plug flow, no radial gradients, uniform adsorbent and catalyst packing and ideal gas. The reaction kinetics models are taken from Xu and Froment [16] and the constants in Eqs. (4) and (6) are found by non-linear parameter estimation with an in-house code. The regressed parameters are given in Table 1.

A hydrotalcite derived Ni catalyst has been used as the steam reforming catalyst due to its high activity and stability [12]. Selected properties of the prepared catalyst are listed in Table 2.

The component balances can be expressed in terms of mole fractions as:

$$\begin{aligned}\frac{\partial y_i}{\partial t} &= D_{\mathrm{L}}\left(\frac{\partial^2 y_i}{\partial z^2} + \frac{1}{P}\frac{\partial P}{\partial z}\frac{\partial y_i}{\partial z} - \frac{1}{T}\frac{\partial T}{\partial z}\frac{\partial y_i}{\partial z}\right) \\ &\quad - \frac{u}{\varepsilon}\left(\frac{\partial y_i}{\partial z} + \frac{y_i}{P}\frac{\partial P}{\partial z} - \frac{y_i}{T}\frac{\partial T}{\partial z}\right) \\ &\quad + \frac{\rho_{\mathrm{b,cat}}RT}{\varepsilon P}\sum_{j=1}^{3}\nu_{ij}\eta_j R_j - \frac{\rho_{\mathrm{b,ad}}RT}{\varepsilon P} r_{\mathrm{ad},i} + \frac{y_i}{T}\frac{\partial T}{\partial t}\end{aligned} \tag{8}$$

where the indices i stands for the components CH_4, CO, CO_2, H_2, N_2 and H_2O, and j stands for the three reactions referred in Eqs. (2)–(4). Making a total of six differential equations. Effectiveness factors are used for the reforming reactions to account for internal diffusion resistance. The effectiveness factors are found from simulations of one catalyst pellet with typical bulk gas phase compositions as boundary conditions, and were found to be 0.8, 0.2 and 0.5 for the reactions referred in Eqs. (2)–(4), respectively.

Table 1
Regressed parameters of the kinetic model for the absorption of CO_2 in lithium zirconate

k^0_{ad} [m^{3n}/(mol^ns)]	n	E_{ad} (J/mol)
4.9×10^{-5}	1.93	8.94×10^{4}

Table 2
Selected properties of the hydrotalcite derived Ni catalyst

Ni loading (%)	Crystal size[a] (nm)	Dispersion[b] (%)	Surface area[c] ($\mathrm{m^2/g}$)
40	12	9	134

[a] By means of XRD.
[b] By means of H_2 chemisorption.
[c] By means of BET.

The axial dispersion coefficient is given by Edwards and Richardson as [17]:

$$D_{\mathrm{L}} = 0.73 D_{\mathrm{m}} + \frac{0.5 u d_{\mathrm{p}}}{1 + 9.49 D_{\mathrm{m}}/(u d_{\mathrm{p}})} \tag{9}$$

The pressure drop in the reactor is calculated from Ergun's equation:

$$\frac{\partial P}{\partial z} = -K_{\mathrm{D}}u - K_{\mathrm{V}}u|u| \tag{10}$$

K_{D} and K_{V} are constants for the viscous and kinetic pressure drop and are given as [18]:

$$K_{\mathrm{D}} = \frac{150\mu(1-\varepsilon)^2}{d_{\mathrm{p}}^2\varepsilon^3} \tag{11}$$

$$K_{\mathrm{V}} = \frac{1.75(1-\varepsilon)}{d_{\mathrm{p}}\varepsilon^3} \tag{12}$$

The energy equation can be formulated in terms of temperature as:

$$\begin{aligned}&\frac{\partial}{\partial t}(\rho_{\mathrm{g}}\mathrm{Cp_g}\varepsilon T + \rho_{\mathrm{b}}\mathrm{Cp_s}T) \\ &\quad = \frac{\partial}{\partial z}\left(\lambda_z\frac{\partial T}{\partial z}\right) - \frac{\partial}{\partial z}(\rho_{\mathrm{g}}u\mathrm{Cp_g}T) - \rho_{\mathrm{b,ad}}\Delta H_{\mathrm{ad}}r_{\mathrm{ad}} \\ &\qquad + \sum_{i=1}^{3}\Delta H_{R_i}\rho_{\mathrm{b,cat}}R_i + \frac{4U}{d_{\mathrm{t}}}(T_{\mathrm{w}} - T)\end{aligned} \tag{13}$$

The effective axial conductivity is calculated from [19]:

$$\frac{\lambda_z}{\lambda_{\mathrm{g}}} = \frac{\lambda_z^0}{\lambda_{\mathrm{g}}} + 0.75(Pr)(Re_{\mathrm{p}}) \tag{14}$$

$$\frac{\lambda_z^0}{\lambda_{\mathrm{g}}} = \varepsilon + \frac{1-\varepsilon}{0.139\varepsilon - 0.0339 + 2/3(\lambda_{\mathrm{g}}/\lambda_{\mathrm{p}})} \tag{15}$$

The bed void fraction is calculated from a relationship given by Dixon [20]:

$$\varepsilon = 0.4 + 0.05\left(\frac{d_{\mathrm{p}}}{d_{\mathrm{t}}}\right) + 0.412\left(\frac{d_{\mathrm{p}}}{d_{\mathrm{t}}}\right)^2 \tag{16}$$

Boundary conditions used in the simulations are:

$$\left(\varepsilon D_{\mathrm{L}}\frac{\partial y_i}{\partial z}\right)_{z=0} = u(y_{\mathrm{f}i} - y_i)$$

$$\left(\varepsilon\lambda_z\frac{\partial T}{\partial z}\right)_{z=0} = \mathrm{Cp_g}uC(T_{\mathrm{f}} - T)$$

$$\left(\frac{\partial y_i}{\partial z}\right)_{z=L} = 0$$

$$\left(\frac{\partial T}{\partial z}\right)_{z=L} = 0$$

A 12 m long tubular reactor with 0.1 m of diameter is simulated. The reactor is fed with steam (97 mol%) and a small amount of hydrogen (3 mol%) at start-up in order to avoid the oxidation of the nickel catalyst [21]. The gas fed in the reaction step is a mixture of steam and methane, with a steam to methane ratio of 6.

The equations are discretised using finite differences. First order upwind differences are used for the convective terms and second order central differences are used for the diffusive terms. The resulting set of equations is solved simultaneously in MATLAB by the method of lines [22] with integration in time. A built-in function in MATLAB, ODE15s, is used for the time integration. ODE15s is a function for the integration of stiff sets of differential and algebraic equations, it employs a variable order NDF (numerical differentiation formulas) integration routines with quasi-constant step size [23].

4. Results and discussion

The crystalline structure of the prepared sample was characterised by XRD analysis. Tetragonal Li_2ZrO_3 was identified as the main phase. The crystal size calculated according to the Scherrer equation is approximately 20 nm.

Fig. 1 shows the CO_2 sorption uptake and regeneration curve of the Li_2ZrO_3 at 873 K. As shown, pure lithium zirconate can take up CO_2 in an amount equivalent to 22 wt.% sample weight and complete absorption is reached within only 10 min. These results present an important improvement of the carbon dioxide sorption rate reported so far. Ida et al. [9] carried out a detailed study on the sorption properties of pure and modified lithium zirconate prepared by a solid-state reaction. According to their investigations, pure lithium zirconate needs more than 24 h to reach 18 wt.% of capacity when the absorption took place at 873 K [9]. Doping of Li/K carbonate on lithium zirconate improved the CO_2 sorption rate considerably; in this case modified Li_2ZrO_3 could adsorb 18 wt.% sample weight within 40 min at 923 K. Nakagawa and Ohashi [5] have reported similar results. Ida and Lin [10] have studied the effect of Li_2CO_3/K_2CO_3 dopant on the CO_2 sorption rate. Doping of Li_2CO_3/K_2CO_3 into Li_2ZrO_3 increases the sorption rate because of the formation of an eutectic molten carbonate at high temperatures. This molten carbonate can considerably reduce CO_2 diffusion resistance compared to the pure Li_2ZrO_3. However, the sorption rate of the pure lithium zirconate prepared in our laboratory is more than three times higher than the sorption rate of the reported Li/K modified Li_2ZrO_3 [5,9,10].

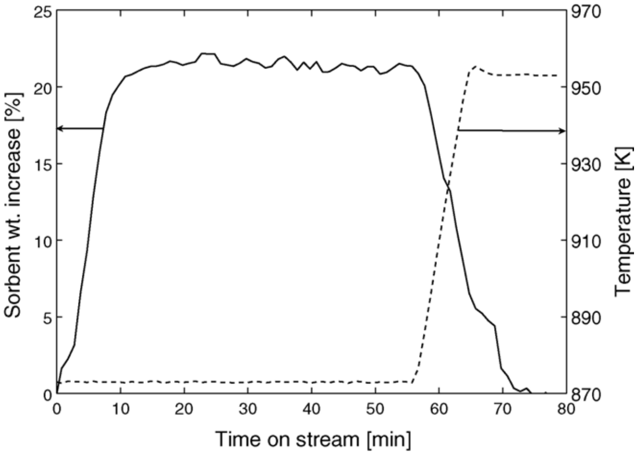

Fig. 1. CO_2 sorption uptake and regeneration curve of the Li_2ZrO_3 at 873 K and P_{CO_2} of 1 atm. Total flow: 100 ml/min.

The sorption curves in Figs. 2 and 3 show the relative weight changes due to absorption of CO_2 at different carbon dioxide partial pressures and two different temperatures: 823 and 848 K, respectively. The extent of the reaction, x, is in this case plotted versus the sorption time and the maximum uptake is set to 0.22 g CO_2/g adsorbent. As can be observed from the figures, the empirical sorption kinetic model presented in Eq. (4) fits reasonably well in the range of CO_2 partial pressures and temperatures that were studied in this work. These modeling results indicate a reaction order of 2

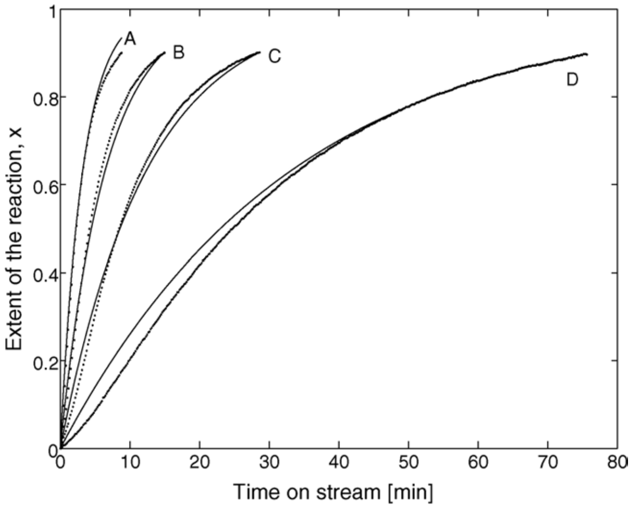

Fig. 2. Comparison of experimental (···) and simulated extent of reaction, x (—) of the CO_2 sorption on Li_2ZrO_3 at 823 K when P_{CO_2} is: (A) 1, (B) 0.7, (C) 0.5 and (D) 0.3 atm, respectively.

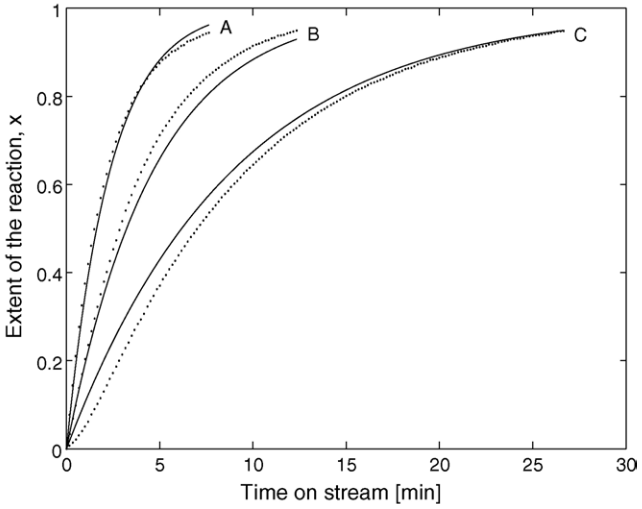

Fig. 3. Comparison of experimental (· · ·) and simulated extent of reaction, x (—) of the CO_2 sorption on Li_2ZrO_3 at 848 K when P_{CO_2} is: (A) 1, (B) 0.7 and (C) 0.5 atm, respectively.

Table 3
Constants used in the model of the reactor

d_p (m)	d_t (m)	L (m)	Cp_s (J/kg)	T_f (K)	T_w (K)
0.005	0.1016	12	850	848	848

P_f (atm)	$\rho_{b,ad}$ (kg/m^3)	$\rho_{b,cat}$ (kg/m^3)	λ_p (w/mK)	N_f (mol/s)
5	596	140	50	0.02

for the CO_2 absorption, which might point out a complicated mechanism of CO_2 in lithium zirconate and a detailed study is in progress. However, as a result, the predicted kinetics of the sorption at low carbon dioxide partial pressures are very slow, due to its second order for CO_2.

The CO_2 sorption kinetic results have been used as input in the dynamic one-dimensional pseudo-homogenous reactor model described above. Fig. 4 shows typical simulated concentration profiles (mole fractions) of different effluent gases on dry basis. The working conditions are summarised in Table 3. The results in Fig. 4 show that in the presence of the CO_2 adsorbent at these working conditions, a H_2 concentration of 95 mol% on dry basis can be reached with CO concentrations lower than 0.2 mol%. Other reactor conditions have also been simulated to evaluate the effects of changes in the conditions. The conversion is sensitive to the steam to carbon ratio, a change from a ratio of 6–4 implies a change in hydrogen purity at the outlet from 95.5 to 90 mol% with a decrease in the conversion from 87 to 70%. Other changes in the conditions were also simulated with a constant S/C ratio of 6. An increase in the flow of methane through the reactor from 0.02 to 0.05 mol/s leads to a decrease in the hydrogen purity from 95.5 to 94 mol%, and in the conversion from 87 to 83%. The same trend is observed if a shorter reactor is used: a 6 m long reactor will give a hydrogen purity of about 94 mol%. Accordingly, the last half of the reactor only increases the purity of the hydrogen by 1.5 mol%. An analysis of the sensitivity of the catalysts effectiveness factors for SERP has also been done, and in addition to the estimated factors used, 1 and 0.1 for all reactions were simulated. The results show that these changes in the effectiveness factor have little or no effect on the conversion. This is because the adsorption is the limiting step in the process, and the steam reforming will be sufficiently fast even with internal diffusion resistance. The effect of the axial dispersion term has been also studied. This term is usually not important in the conventional steam-reforming. Still, this term was included for the simulation of the sorption enhanced reaction process due to the low space velocities that are used in this case. However, simulations show that the axial dispersion has little or no effect on the solution and could be neglected.

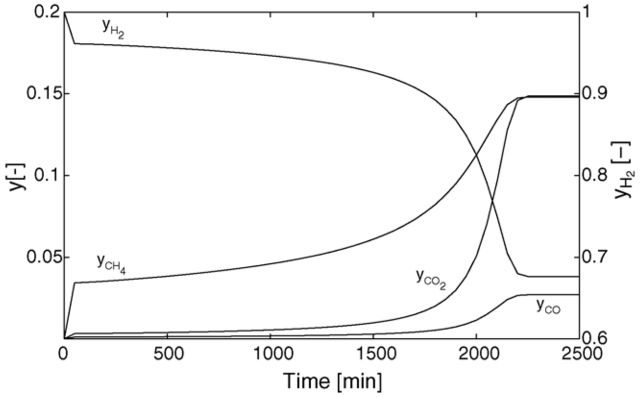

Fig. 4. Simulation of the reactor effluent concentration profiles on a water-free basis. Reaction conditions: T_f = 848 K, P_f = 5 atm, steam to carbon ratio = 6, N_f = 0.02 mol/s.

Summarising, higher conversion, and as consequence purer hydrogen, is enhanced by using long residence times in the reactor, which implies that the working capacity of the process can be low compared to traditional steam reforming. To be able to increase the productivity, the kinetics of the adsorbent at low carbon dioxide partial pressures have to be improved. Introducing several promoters such as Mg and K has been reported to considerably improve the performance of the sorbent kinetics [6,24]. Promotion may consequently increase the throughput potential of the process.

5. Conclusion

A sorption enhanced reaction process has been modelled for direct production of a rich hydrogen-containing stream. Lithium zirconate and a hydrotalcite derived Ni catalyst have been used as sorbent and catalyst, respectively. The process is capable of directly producing concentrations of H_2 larger than 95 mol% with methane as the main side product with less than 0.2 mol% of CO. After sorbent saturation the conversion of methane follows the thermodynamics and kinetics of a conventional steam reforming process. SERP opens new opportunities for the production of nearly CO free H_2. In addition, lithium zirconate has been demonstrated to be an appropriate material for SERP showing high adsorption capacity. However, improvements in the operating capacity of the process are still possible by enhancing the sorption properties of the materials at low CO_2 concentrations.

Acknowledgement

The Research Council of Norway (NFR) is thanked for financial support.

References

[1] E.L. Draper, R. Becker, The National Coal Council, Washington, DC, 2000.
[2] C.H. Liao, M.H. Li, Chem. Eng. Sci. 57 (2002) 4569.
[3] R.V. Siriwardane, M.S. Shen, E.P. Fisher, Energy Fuels 15 (2001) 279.
[4] K. Kuraoka, N. Kubo, T. Yazawa, J. Sol–Gel Sci. Technol. 19 (2000) 515.
[5] K. Nakagawa, T. Ohashi, J. Electrochem. Soc. 145 (1998) 1344.
[6] K. Nakagawa, T. Ohashi, Electrochemistry 67 (1999) 618.
[7] B.N. Nair, T. Yamaguchi, H. Kawamura, S.I. Nakao, J. Am. Chem. Soc. 87 (2004) 68.
[8] R. Xiong, J. Ida, Y.S. Lin, Chem. Eng. Sci. 58 (2003) 4377.
[9] J. Ida, R. Xiong, Y.S. Lin, Sep. Purif. Technol. 36 (2004) 41.
[10] J. Ida, Y.S. Lin, Environ. Sci. Technol. 37 (2003) 1999.
[11] B. Balasubramanian, A.L. Ortiz, S. Kaytakoglu, D.P. Harrison, Chem. Eng. Sci. 54 (1999) 3543.
[12] K.O. Christensen, Steam reforming of methane on different Ni catalysts, Doctoral thesis, NTNU, Trondheim, 2005, p. 46.
[13] D. Chen, E. Ochoa-Fernández, M. Rønning, T. Grande, Patent (2005), O.nr. 110520.
[14] H.P. Klug, L.E. Alexander, X-ray diffraction procedures for polycrystalline and amorphous materials, Wiley, New York, 1954.
[15] D. Chen, H.P. Rebo, K. Moljord, A. Holmen, Chem. Eng. Sci. 51 (1996) 2687.
[16] J. Xu, G.F. Froment, AIChE J. 35 (1989) 88.
[17] M.F. Edwards, J.F. Richardson, Chem. Eng. Sci. 23 (1968) 109.
[18] S. Ergun, Chem. Eng. Prog. 48 (1952) 89.
[19] S. Yagi, D. Kunii, N. Wakao, AIChE J. 6 (1960) 543.
[20] A.G. Dixon, CJChE 66 (1988) 705.
[21] T. Sperle, D. Chen, R. Lødeng, A. Holmen, Appl. Catal. A. 282 (2005) 195.
[22] W.E. Schiesser, The Numerical Method of Lines: Integration of Partial Differential Equations, Academic Press, 1991.
[23] L.F. Shampine, M.W. Reichelt, Siam J. Sci. Comput. 18 (1997) 1.
[24] T. Ohashi, K. Nakagawa, Mater. Res. Soc. Symp. Proc. 547 (1999) 249.